



# Design and Simulation of Multiband Terahertz Metamaterial Absorber

T.R.Ganesh Babu<sup>1</sup>, P.Sukumar<sup>2</sup>, R.Usha<sup>3</sup>, R.Praveena<sup>1</sup>

<sup>1</sup>Muthayammal Engineering College, Salem, Tamil Nadu, India

<sup>2</sup>Nandha Engineering College, Erode, Tamil Nadu, India

<sup>3</sup>S.A Engineering College, Chennai, Tamil Nadu, India

ganeshbabutr@gmail.com, sukumarwin@gmail.com, ushar@saec.ac.in,  
praveenajuhi@gmail.com

**Abstract.** This paper presents the design and simulation of a multiband metamaterial absorber. This Meta material absorber covers the 6 to 16 GHz frequency band. The size of the unit cell and other geometrical dimensions such as the radius and width of the rings are optimized so that the absorptions occur at three different frequencies of 9.0187 GHz, 0.99926 GHz and 13.367 GHz. Numerical simulation of the designed structure is evaluated using CST Software Microwave Studio. The goal is to design a Metamaterial absorber in terahertz applications. It provides fast and secure communication, better penetration depth and less scattering, good spatial imaging resolution, non-ionizing, intra and interparticle modes of many molecules lie in this range.

**Keywords:** Metamaterial, Multiband, Terahertz, Absorption rate, permittivity.

## 1 Introduction

The word "metamaterial" is derived from the Greek word meta, meaning "beyond". It was first introduced by R.M.Walser. Metamaterials are artificially created new classes of materials that do not occur in nature. These materials have unusual electromagnetic (EM) properties with values of effective permittivity and permeability less than zero that are not observed in naturally occurring materials [1]. The geometry, periodic arrangement, and orientation of the structural units give rise to unusual electromagnetic properties.

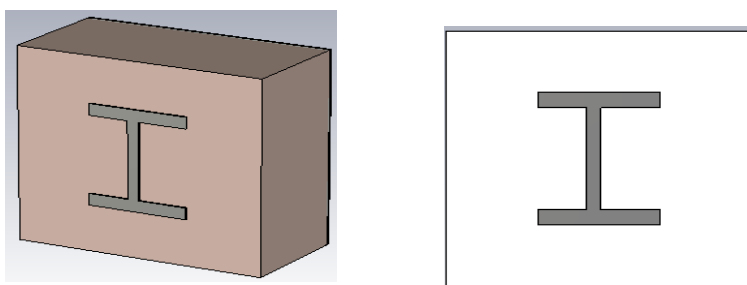


**Fig. 1.** Proposed MMA Perspective and front view

© The Author(s) 2024

R. Murugan et al. (eds.), *Proceedings of the International Conference on Signal Processing and Computer Vision (SIPCOV 2023)*, Advances in Engineering Research 239,

[https://doi.org/10.2991/978-94-6463-529-4\\_36](https://doi.org/10.2991/978-94-6463-529-4_36)

These unusual electromagnetic properties are not inherited from the composition of the material. permittivity and permeability less than zero. Metamaterials can be defined as periodic arrangements or irregular periodic arrangements of subwavelength metallic structures that derive the properties of electromagnetic materials from their geometry rather than inheriting them directly from the material composition or band structure which is shown in figure 1. Electromagnetic properties of materials are characterized based on negative or positive values of permittivity or permeability. Most materials found in nature have positive values of permittivity and permeability and are therefore called "double positive" (DPS) materials. These materials fall into the first quadrant and the energy flow carried by the electromagnetic wave is determined by the direction vector 's'. Materials showing negative values of permittivity or permeability are referred to as single negative and are further divided into two categories, "epsilon-negative" (ENG) and "mu-negative" (MNG). These materials fall into the second and fourth quadrants. When both permittivity and permeability are positive, the refractive index is positive and has a real value that allows light to propagate. When either of these two parameters is negative,  $n$  becomes an imaginary inhibiting wave generation. When both are negative, the index of refraction is negative, but a real value that allows the wave to propagate in the opposite direction.

## 2 Related Work

Wangyang Li, Yongzhi cheng, 'Dual-band tunable terahertz perfect metamaterial absorber based on strontium titanate (STO) vol. 462, pp. 125265, 1 May 2020. This dual-band MMA is a simple periodic array [2] consisting of two stacked square-shaped STO resonator structures and a copper substrate. These STO material-based MMAs usually require unit cells with a complex sandwich structure, resulting in increased manufacturing difficulty and cost.

Ben-Xin Wang, Gui-Zhen Wang, Tian Sang, Ling-Ling Wang, "Six-band terahertz metamaterial absorber based on the combination of multi-order responses of metal patches in a two-layer layered resonance structure", Scientific Reports, vol. 14, pp. 41373, 2017. The numeric MMA absorber is realized by integrating two multiple studies of a six-band metamaterial absorber composed of two alternating layers of metallic-dielectric layers on top of a continuous metallic plane. The two gold layers are separated by several dielectric layers (polyimide).

Dutta, R, Bakshi, SC & Mitra, D, 'Ultrathin Compact Polarization-Insensitive HeptaBand Absorber', IMArc, Kolkata, India, pp. 1-4, 2018. An ultrathin, compact, heptaband microwave MMA is designed for the first. The MMA band structures nested within each other. An ultrathin, compact, [13] heptaband metamaterial absorber (MMA) is designed for the first time. The MMA absorber is realized by integrating two multi-band MMA structures nested inside each other. The novelty of the proposed structure lies in its fourfold symmetry, which allows it to be a polarization-insensitive absorber.

## 3 Methodology

A multi-band terahertz metamaterial absorber is designed without the use of stacked layers and multiple resonators in a single unit cell, and the numerical simulation of the structure is evaluated using CST Microwave studio software. The reference structure consists of two copper layers with a thickness of 0.035 mm separated by a dielectric layer. The top copper layer consists of three 7-sided ngon patches with a copper conductivity of  $5.8 \times 10^{-7}$ . The back copper layer  $\epsilon$  of the reference structure is completely copper, separated from the top layer by a single-layer dielectric [3]. The dielectric material is an FR-4 substrate with a thickness of mm and  $\epsilon_r = 4.05$  and  $\tan \delta = 0.02$ . The top layer of the reference structure with dimensions; The length of the patch is 5 mm, the width of the patch is 5 mm. A shift method used to demonstrate that by increasing the dimensions and size of a structure by 100%, the 0-frequency response of the structure can be shifted by half the frequency.

$$\epsilon_r = n^2 - k^2$$

$$\tan \delta = \frac{(2nk)}{(n^2 - k^2)}$$

From the above, we get that by changing the dimensions of the structure, a shift in the frequency response can be achieved. Although changing the size of the structure results in a change in the frequency response band, and changing the dimensions of the structure changes the band response at lower or higher frequencies or both [4]. The dielectric material is an FR-4 substrate with a thickness of mm and  $\epsilon_r = 4.05$  and  $\tan \delta = 0.02$ . The top layer of the reference structure with dimensions; The length of the patch is 5 mm, the width of the patch is 5 mm. The proposed structure has only three layers, namely the ground plane, the dielectric substrate and the top patch. Here, the Top patch has a very simple structure. So, in terms of production, it will be easy. The first "I Shaped" patterned layer is critical in the MMA design [5] because it can be tuned to meet the impedance matching condition of the environment and achieve zero reflection at resonant frequencies as shown in figure 2.

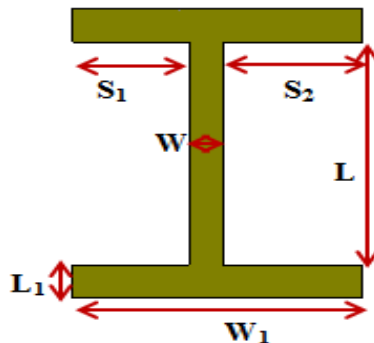
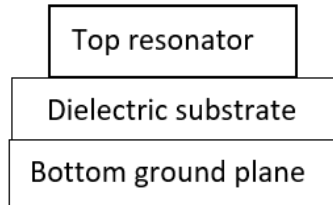


Fig. 2. I-Shaped MMA

The second dielectric layer is a spacer used to dissipate the EM wave and the metal base layer blocks all incident EM waves in below figure 3.



**Fig. 3.** Three layers of MMA

The parameters of the unit are shown in the figures below. The length and width of the resonator ( $L \times W$ ) is  $(0.2 \times 0.023)$  mm and the length and width of the resonator ( $L1 \times W1$ ) is  $(0.03 \times 0.2)$  mm [6]. The length of  $s1$  and  $s2$  is 0.097 mm and 0.08 mm shown in below table 1.

**Table 1.** Parameters of MMA

| Parameters   | Values(mm)           |
|--|----------------------|
| Length and width of the resonator ( $L \times W$ )   | $(0.2 \times 0.023)$ |
| Length of the $s1$ and $s2$                          | 0.097 & 0.08         |
| Length and width of the resonator ( $L1 \times W1$ ) | $(0.03 \times 0.2)$  |

A flowchart of the unit cell design process is shown in the figure 4 below. In this process, unit cell, tri-layer unit cell arrangement and substrate material: Fr-4 are considered as three initial inputs. The reason is a decision based on a literature review and other considerations that are limited in this project [7]. In the modification process, the physical parameters include the three basic parameters of the n-gon shaped patch "l", "w" and "d" in each layer as well as the thickness of the substrate.

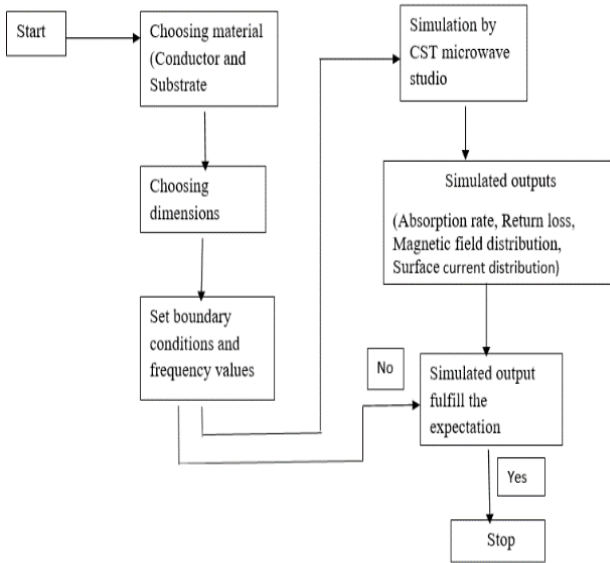


**Fig. 4.** Flow chart of unit cell design process

Our MMA is three layers, two of which are metal and are made of copper and the other is a dielectric which is made of fr-4. A copper patch with a 3\*7-sided 7- sided ring and a conductivity of  $5.8 \times 10^{-7} \epsilon/\epsilon$  is attached to the upper front and back of the structure. The front patch layer and the full copper laminated back were separated using FR4, a material that is a good candidate for MMA fabrication. The front patch layer and the full copper laminated back were separated using FR4, a material that is a good candidate for MMA fabrication.

In order to increase the number of bands and higher absorption, the MMA design is developed [8]. In this, four L-shaped resonators were placed along with an I-shaped resonator in figure 5. So, the developed MMA gives 2 extra bands.

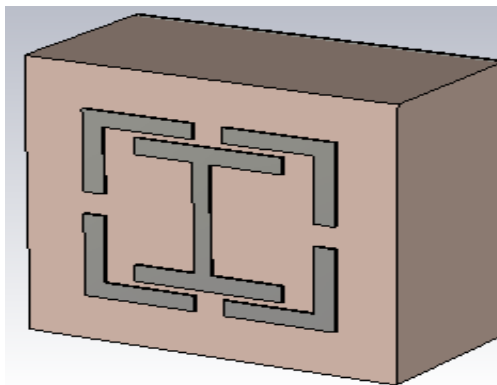


**Fig. 5.** Developed MMA

So, from this developed absorption structure, we achieved five absorption bands with a higher absorption rate [8].

### Stages of developing MMA

#### Stage 1

The figure 6 shows the shapes which is used to design MMA.

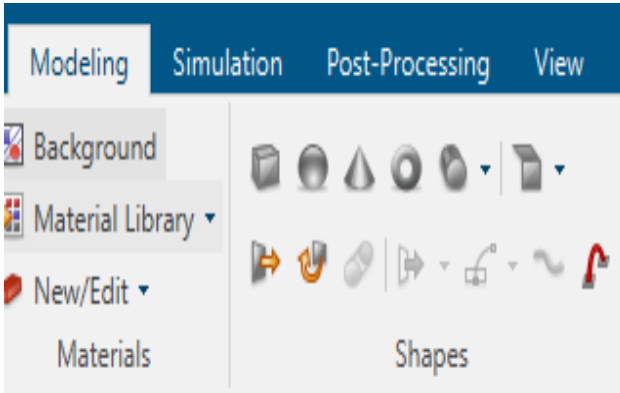


Fig. 6. Shapes Used to design MMA

#### Stage 2

Below figure 7 shows the initial conditional settings of MMA.

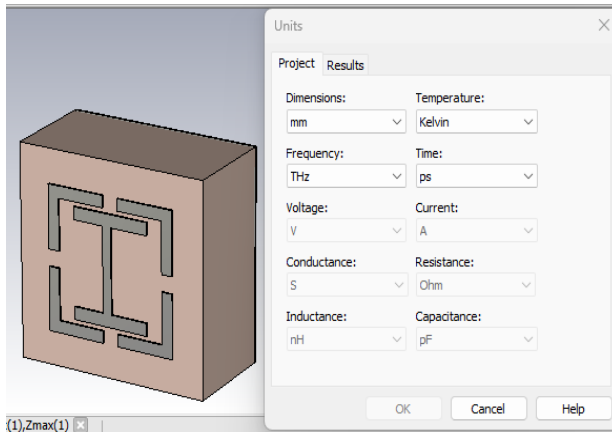


Fig. 7. Initial conditional settings of MMA

### Stage 3

Below figure shows how to take the boundary conditions to design MMA.

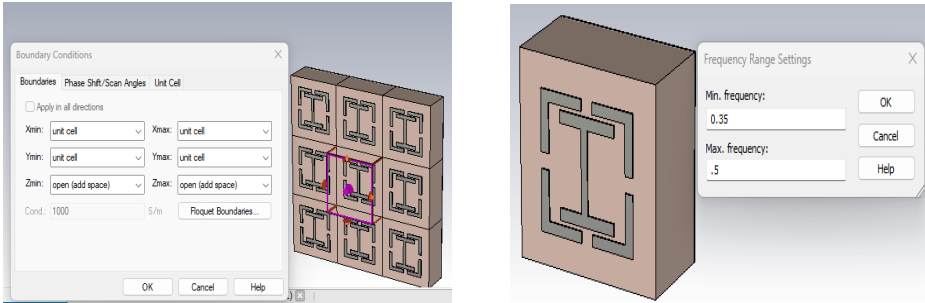


Fig. 8. Boundary Conditions of MMA

### Stage 4

Figure 9 shows the frequency range of MMA

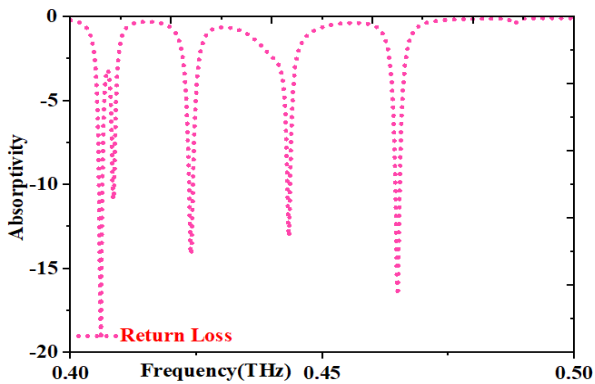


Fig. 9. Frequency range of MMA

## 4 Results and Discussion

The graph below shows the absorption rate (y-axis) of the proposed MMA in terms of frequency (x-axis). The proposed MMA resonates at five frequencies of 0.42, 0.425, 0.43, 0.44 and 0.46 THz with an absorption rate of 99.5, 97.9, 99.1, 98.9, and 99 respectively [9]. Chart drawn using origin pro software.

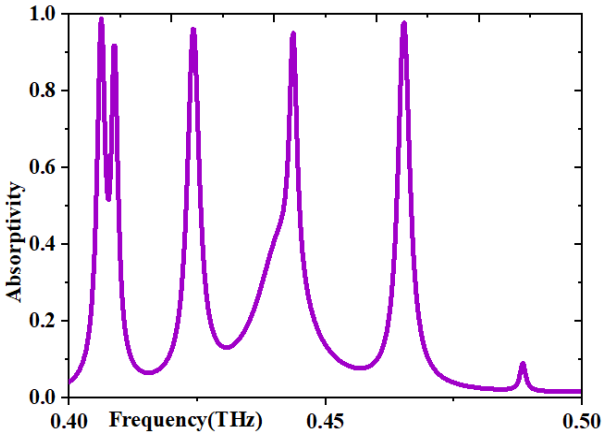


Fig. 10. Absorption rate curve in terms of Frequency.

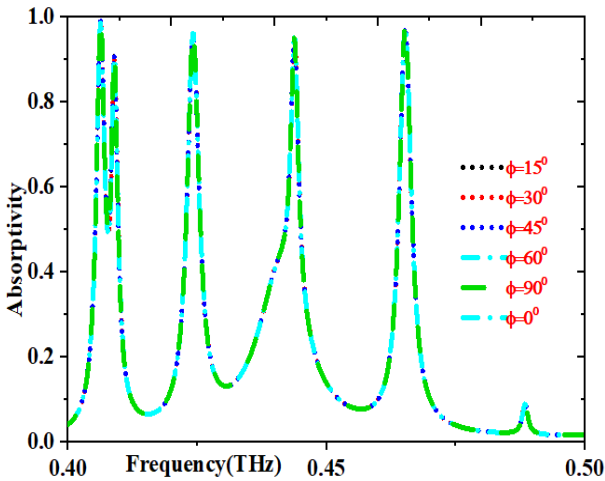
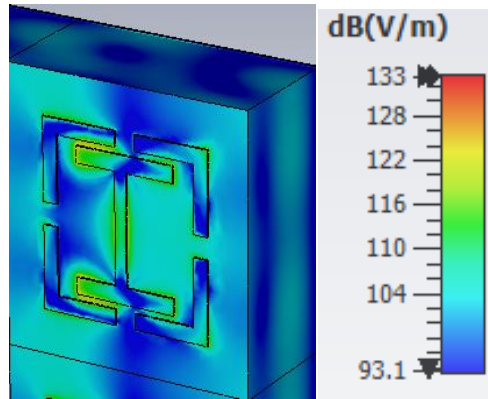


Fig. 11. Return Loss Curve in terms of Frequency

The graphs 10 and 11 above shows the loss of return (y-axis) of the proposed MMA in terms of frequency (x-axis). The proposed MMA resonates at five frequencies of 0.42, 0.425, 0.43, 0.44 and 0.46 THz with a return loss of -18, -11, -14.5, -14, -17 Db [10]. This electric field distribution and magnetic field distribution occur at 0.42 THz, 0.425 THz, 0.43 THz, 0.44 THz, and 0.46 THz, respectively. The figures below show how the electrical and magnetic separation occurs.





**Fig. 12.** Electric Field distribution

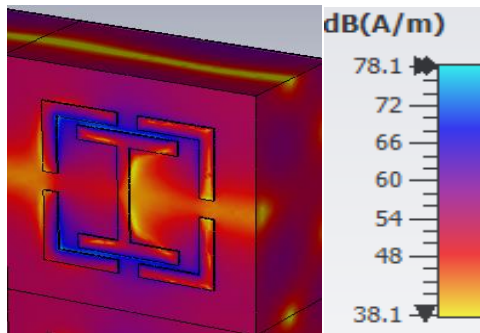


**Fig. 13.** Magnetic Field Distribution

The above figures 12 & 13 shows how the electric and magnetic distributions will occur.

The electromagnetic field is a physical behaviour that arises in space due to the influence of time-varying electric charges and represents the interaction between electric and magnetic fields. Unlike static charges, which can only produce static electric fields in space, time-varying electric charges are one of the sources for the formation of magnetic fields, which in turn produce time-varying electric fields.

In the environment, there are two main quantities, also known as constitutive parameters, namely the electrical permittivity and the magnetic permeability [11], in addition to the conductivity, which determines the nature of the electromagnetic wave and its behaviour in the environment. In other words, the above parameters together with the boundary conditions in the medium clearly determine the response of such a medium to an incoming electromagnetic wave which shown below figure 14. The absorption and resonant frequencies of the structure did not change when the values of  $\phi$  changed due to the symmetrical nature of the structure [12]. Therefore, the proposed MMA exhibits excellent polarization-independent absorption performance.

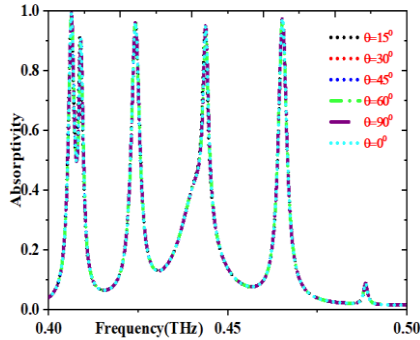


Fig. 14. Simulation on different Pi and Theta angles

## 5 Conclusion

The MMA is designed using only three layers without the use of stacked layers and multiple resonators in a single unit cell with a frequency range from 0.4 THz to 0.5 THz. Within a small frequency range, three non-overlapping curves can be obtained at 0.4 THz, 0.468 THz, 0.4928 THz with absorption rates of 99.3%, 97.9%, 99.1%, 98.9% and 99.1%. The simulated output is drawn using origin pro software. Return losses, electric and magnetic field distributions, and surface current distribution plots for all five frequencies are analysed.

## References

1. Ben-Xin Wang, Gui-Zhen Wang, Tian Sang, Ling-Ling Wang, "Six-band terahertz metamaterial absorber based on the combination of multi-order responses of metal patches in a two-layer layered resonance structure", *Scientific Reports*, vol. 14, pp. 41373, 2017.
2. Dutta, R, Bakshi, SC & Mitra, D 2018, 'Ultrathin Compact Polarization-Insensitive Hepta-Band Absorber', *IMaRC*, Kolkata, India, pp 1-4.
3. Cheng, Y, Zou, Y, Luo, H, Chen, F & Mao, X 2019, 'A compact ultrathin seven-band microwave metamaterial absorber based on a simple resonator structure', *Journal of Electronic Materials*, vol. 48, pp. 0.3939–3946.
4. Boyang Zhang, Joshua Hendrickson, and Junpeng Guo, "Multispectral near-perfect metamaterial absorbers using spatially multiplexed metal square plasmon resonance structures," *Journal of the Optical Society of America B*, vol. 30, pp. 656-662, 2013.
5. Cheng, Y., Nie, Y., & Gong, R,' A polarization-insensitive and omnidirectional broadband terahertz metamaterial absorber based on coplanar multi-square films, *Optics & Laser Technology*, vol. 48, pp. 415–421, 2013.
6. Liu, S., Chen, H., & Cui, T. J, 'Broadband terahertz absorber using multilayer stacked rods', *Applied Physics Letters*, 106(15), 151601, 2015.
7. Fan, J., Xiao, D., Wang, Q., Liu, Q., & Ouyang Z, 'Wide-angle broadband terahertz metamaterial absorber with multilayer heterostructure', *Applied Optics*, vol.56 (15), p.4388, 2017 .
8. X. Shen et al., "Polarization-Independent Wide-Angle Triple-Band Metamaterial Absorber," *Opt. Exp.*, Vol. 19, pp. 9401–9407, 2011.

9. X. Shen et al., "Triple-Band Terahertz Metamaterial Absorber: Design, Experiment, and physical interpretation," *Appl. Phys. Lett.*, Vol. 101, 2012.
10. S. Liu et al., "Two-Layer Four-Band Metamaterial Absorber in Terahertz" Frequencies", *J. Appl. Phys.*, vol. 118, 2015.
11. D. R. Chowdhury et al., "Broadband planar terahertz metamaterial with embedded Structure", *Opt. Exp.*, vol. 19, pp. 15817-15823, 2011.
12. S. Cao et al., "Meta-microwind Mill Structure with Multiple Absorption Peaks for the Detection of ketamine- and amphetamine-type stimulants in the Terahertz domain", *Opt. Mater. Exp.*, Vol. 4, pp. 1876-1884, 2014.
13. B. X. Wang, "Quad-Band Terahertz Metamaterial Absorber Based on the Combining of dipole and quadrupole resonances of two SRRs," *IEEE Journal of Selected Topics in Quantum Electronics*, Vol. 23, No. 4, pp. 1-7, 2017.
14. H. Y. Meng et al., "A simple design of a multiband terahertz metamaterial Absorber based on a periodic square metal layer with a T shape Gap, *Plasmonics*, vol. 13, No. 1, pp. 269-274, 2018.
15. M. Gupta, Y. K. Srivastava, and R. Singh, "A Toroidal Metamaterial Switch," *Adv. Mater.*, vol. 30, No. 4, pp. 1-8, 2018.

**Open Access** This chapter is licensed under the terms of the Creative Commons Attribution-NonCommercial 4.0 International License (<http://creativecommons.org/licenses/by-nc/4.0/>), which permits any noncommercial use, sharing, adaptation, distribution and reproduction in any medium or format, as long as you give appropriate credit to the original author(s) and the source, provide a link to the Creative Commons license and indicate if changes were made.

The images or other third party material in this chapter are included in the chapter's Creative Commons license, unless indicated otherwise in a credit line to the material. If material is not included in the chapter's Creative Commons license and your intended use is not permitted by statutory regulation or exceeds the permitted use, you will need to obtain permission directly from the copyright holder.

